arXiv:1606.08228v1 [cond-mat.stat-mech] 27 Jun 2016

Ising antiferromagnet on the 2-uniform lattices

Unjong Yu
*Department of Physics and Photon Science, Gwangju Institute of Science and Technology, Gwangju 61005, South Korea**

The antiferromagnetic Ising model is investigated on the twenty 2-uniform lattices using the Monte-Carlo method based on the Wang-Landau algorithm and the Metropolis algorithm to study the geometric frustration effect systematically. Based on the specific heat, the residual entropy, and the Edwards-Anderson freezing order parameter, the ground states of them were determined. In addition to the long-range-ordered phase and the spin ice phase found in the Archimedean lattices, two more phases were found. The partial long-range order is long-range order with exceptional disordered sites, which give extensive residual entropy. In the partial spin ice phase, the partial freezing phenomenon appears: Majority of sites are frozen without long-range order, but the other sites are fluctuating even at zero temperature. The spin liquid ground state was not found in the 2-uniform lattices.

PACS numbers: 05.50.+q, 05.10.Ln, 64.60.De, 75.10.Hk

I. INTRODUCTION

Recently, frustration has attracted intensive attention due to unexpected phenomena and exotic order [1–3]. The Ising model [4] always have a long-range-ordered ground state in two and higher dimension without frustration [5]. With frustration, however, it has various ground states such as long-range-ordered phase, spin glass, spin ice, and spin liquid phase [2, 3, 6]. Frustration induced by geometric effect without disorder is called the geometric frustration [7]. In this paper, the geometric frustration is investigated systematically within the antiferromagnetic Ising model on two-dimensional 2-uniform lattices.

In a two-dimensional lattice made by regular polygons, when there exist k kinds of topologically equivalent vertices, it is called k-uniform lattice. When there is only one kind (uniform tiling), it is also called the Archimedean lattice. There are exactly eleven Archimedean lattices, and seven lattices among them are frustrated [8]. The ground state of the antiferromagnetic quantum Heisenberg model was investigated systematically: the kagome and the star lattice were proposed as quantum spin liquid and the other five lattices were classified tentatively as long-range-ordered phase [9, 10]. In the case of the antiferromagnetic Ising model, ground states of them are classified into long-range-ordered phase (Shastry-Sutherland and trellis lattices), spin ice (bounce, maple-leaf, and star lattices), and spin liquid (triangular and kagome lattices), in the order of stronger frustration [6]. Although the Archimedean lattice is a good starting point to study geometric frustration [11], seven lattices are not enough for a systematic study of various frustration effects, and we present study of the frustration effect on the 2-uniform lattices in this work. There exist exactly twenty 2-uniform lattices [8], as are listed in Fig. 1 and Table I. We labeled them from T12 to T31 after eleven Archimedean lattices. Differently from the Archimedean lattices, which have corresponding natural material systems [9, 12], 2-uniform lattices have not been found in nature, yet, but it is expected to become possible to make artificial systems with a 2-uniform structure in the future. At least, we can get an insight for the geometric frustration by systematic study on the 2-uniform lattices.

In this paper, we report detailed study of the antiferromagnetic Ising model on the 2-uniform lattices. Specific heat, residual entropy, and freezing order-parameter are obtained to identify the ground state. Finite temperature phase transitions in weakly frustrated lattices are also investigated.

II. MODEL AND METHOD

The Ising model Hamiltonian in this work is as follows.

$$H = -J \sum_{\langle i,j \rangle} S_i S_j \ . \tag{1}$$

The spin at the i-th site S_i may take the values of $+1$ or -1, only. The summation $\langle i, j \rangle$ runs for all the nearest-neighbor pairs, excluding double counting. The coupling constant J and the Boltzmann constant k_B are set to be $J = -1$ and $k_B = 1$. Only antiferromagnetic interaction is considered within this paper.

The calculation was done for parallelepiped lattices with number of sites $N = B \times L \times L$, where B and L are the number of sites per unit cell and the linear size, respectively. The periodic boundary condition is used. To simulate frustrated systems, we used the Wang-Landau algorithm [13]. The Wang-Landau algorithm calculates the density of states $\rho(E)$ (DOS) as a function of energy E directly by the random walk with the transition probability $P(i \to j) = \min\{1, \rho(E_i)/\rho(E_j)\}$. At each step, the histogram $h(E_i)$ and the DOS $\rho(E_i)$ of the present energy E_i is adjusted by $h(E_i) \to h(E_i) + 1$ and $\rho(E_i) \to f_n \, \rho(E_i)$ with an amplification factor $f_n > 1$

*E-mail me at: uyu@gist.ac.kr

TABLE I: Name, number of lattice points per basis (B), average coordination number (z), antiferromagnetic ground state energy per bond ($E_g^{\rm AF}$), antiferromagnetic transition temperature (T_c), exact residual entropy (S_0), and ground state for each 2-uniform lattice. LRO means long-range order.

	Name	B	z	$E_g^{\rm AF}$	$T_c^{\rm AF}$	S_0	Ground state
T21	$(3^3,4^2;3^2,4,3,4)_2$	8	5	$-3/5$	1.193(1)	$\log(2)$	LRO
T26	$(3^2,6^2;3,6,3,6)$	6	4	$-2/3$	1.182(1)	$\log(2)$	LRO
T13	$(3^6;3^4,6)_2$	8	21/4	$-3/7$	1.076(2)	$\log(2)(1+N/4)$	Partial LRO
T17	$(3^6;3^2,4,12)$	14	30/7	$-3/5$	1.210(1)	$\log(2)(1+N/7)$	Partial LRO
T18	$(3^6;3^2,6^2)$	7	30/7	$-3/5$	1.324(1)	$\log(2)(1+N/7)$	Partial LRO
T14	$(3^6;3^3,4^2)_1$	4	11/2	$-5/11$	0.17(1)	$\log(8)L$	1-direction LRO
T15	$(3^6;3^3,4^2)_2$	3	16/3	$-1/2$	0.27(1)	$\log(4)L$	1-direction LRO
T19	$(3^4,6;3^2,6^2)$	4	9/2	$-5/9$	0	$\log(2)L$	1-direction LRO
T23	$(3^3,4^2;4^4)_1$	3	14/3	$-5/7$	0	$\log(2)L$	1-direction LRO
T24	$(3^3,4^2;4^4)_2$	4	9/2	$-7/9$	0	$\log(2)L$	1-direction LRO
T30	$(3,4^2,6;3,6,3,6)_2$	5	4	$-3/5$	0	$\log(2)(L+N/5)$	Partial 1-direction LRO
T20	$(3^3,4^2;3^2,4,3,4)_1$	12	5	$-7/15$	-	$[0.18472(1)]\,N$	Spin ice
T22	$(3^3,4^2;3,4,6,4)$	12	9/2	$-5/9$	-	$[0.1258(2)]\,N$	Spin ice
T25	$(3^2,4,3,4;3,4,6,4)$	12	9/2	$-5/9$	-	$[0.083(3)]\,N$	Spin ice
T28	$(3,4^2,6;3,4,6,4)$	18	4	$-2/3$	-	$[0.08401(1)]\,N$	Spin ice
T12	$(3^6;3^4,6)_1$	12	11/2	$-13/33$	-	$[0.172(1)]\,N$	Partial spin ice
T16	$(3^6;3^2,4,3,4)$	7	36/7	$-4/9$	-	$[(\log(2)+0.32306595)/7]\,N$	Partial spin ice
T27	$(3,4,3,12;3,12^2)$	8	7/2	$-3/7$	-	$[0.37757(1)]\,N$	Partial spin ice
T29	$(3,4^2,6;3,6,3,6)_1$	5	4	$-3/5$	-	$[0.18376(2)]\,N$	Partial spin ice
T31	$(3,4,6,4;4,6,12)_2$	18	10/3	$-11/15$	-	$[0.12885(2)]\,N$	Partial spin ice

until the histogram $h(E_i)$ becomes flat enough. When the standard deviation of the histogram is less than 4% of its average, the normalization of $\sum_i \rho(E_i) = 2^N$ is performed and a new scan starts with an empty histogram $[h(E_i) = 0]$ and a smaller value of $f_{n+1} = \sqrt{f_n}$.

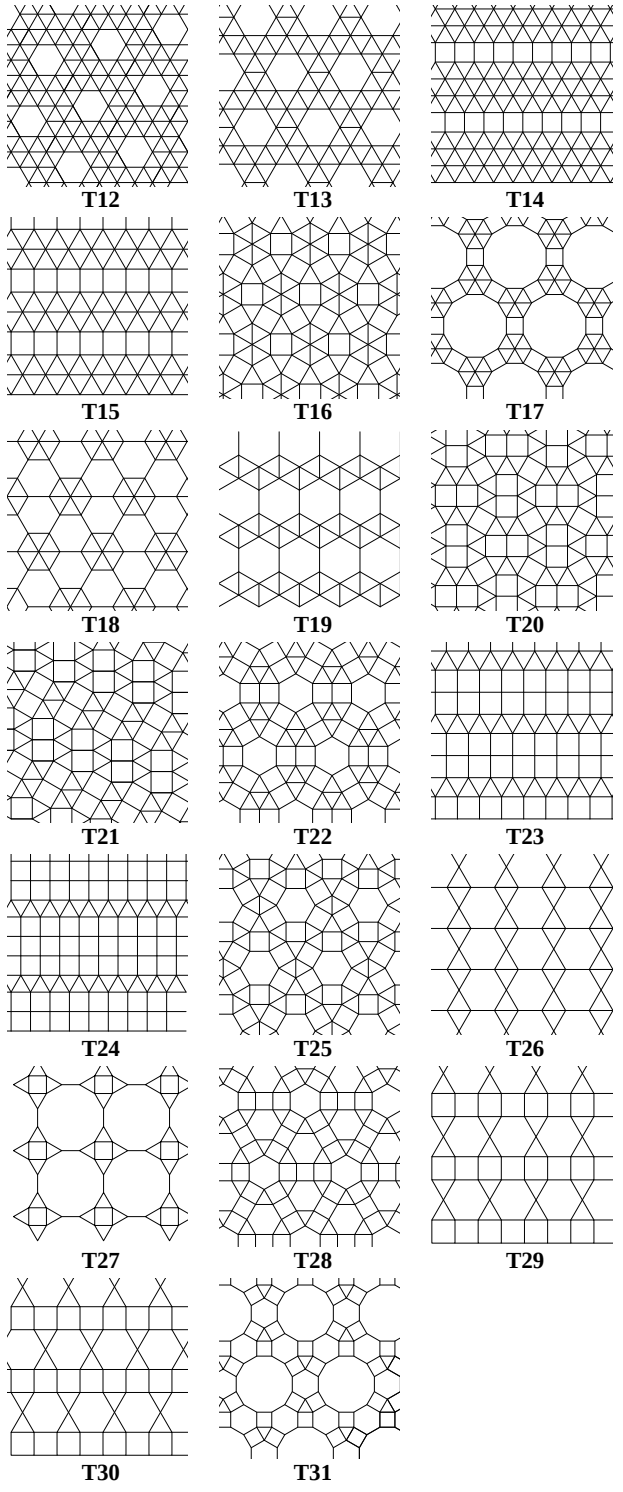

FIG. 1: The twenty 2-uniform lattices.

The whole simulation begins with an initial amplifier $f_0 = e$ and stops when f_n approaches enough to 1: $f_n < \exp(10^{-10})$. If the simulation is successful, the error is expected to be the same order as $\log(f_n)$. Although the Wang-Landau method is slow and can be applied to only small clusters, it gives reliable results for the frustrated systems because it is not stuck to a metastable state. After the DOS $\rho(E)$ is obtained, the specific heat $c(T)$ can be calculated easily as a function of temperature T:

$$c(T) = \frac{1}{T^2}\left\{\langle E^2\rangle_T - (\langle E\rangle_T)^2\right\} \tag{2}$$

$$\text{with} \quad \langle X\rangle_T = \frac{\sum_i X_i\,\rho(E_i)\,e^{-E_i/T}}{\sum_i \rho(E_i)\,e^{-E_i/T}}\ . \tag{3}$$

The residual entropy S_0 can be calculated also directly from the DOS ($\rho(E)$) obtained by the Wang-Landau algorithm: $S_0 = \log[\rho(E_0)]$, where E_0 is the lowest energy. Since the Wang-Landau algorithm can give only static information, we also used the Metropolis algorithm [14] to study fluctuation around a ground state.

III. RESULTS AND DISCUSSION

From the specific heat (Fig. 2) and residual entropy data (Fig. 3) obtained by the Wang-Landau method, eleven lattices were classified to have long-range-ordered ground states. Two of them (T21 and T26) have conventional long-range order with residual entropy $S_0 = \log(2)$, which was confirmed by the Wang-Landau calculation. The degeneracy of two is from the Kramers degeneracy. Other three lattices (T13, T17, and T18) have partial long-range order, which means the long-range order except part of the lattice that keeps disordered even at zero temperature. Therefore, the residual entropy is extensive like the spin ice and the spin liquid. For example, a ground state of lattice T18 is shown in the right panel of Fig. 3(a). Without sites in the center of hexagons, which are represented by red circles, there is no frustration and the ground state is uniquely determined except the Kramers degeneracy. Since the site can have any spin state between up and down, the degeneracy is $W_0 = 2\times 2^{L^2} = 2\times 2^{N/7}$ and the residual entropy becomes extensive: $S_0 = \log(W_0) = \log(2)(1 + N/7)$. In the same way, the residual entropy of T13 and T17 can be understood, too. In the case of T13, two spins out of eight spins in a unit cell are disordered and $S_0 = \log(2)(1 + N/4)$. These behaviors are well confirmed by the Wang-Landau calculations. The partial long-range order has been observed in a number of models with frustration. The classical Heisenberg model with uniaxial exchange anisotropy on the triangular lattice has a partial order, where 2/3 spins make a long-range-ordered honeycomb lattice while the other 1/3 spins are disordered [15]. The body-centered-cubic (bcc) lattice may have the partial order with nearest-neighbor (NN) and next-nearest-neighbor (NNN) interactions, too [16]. The Potts model shows

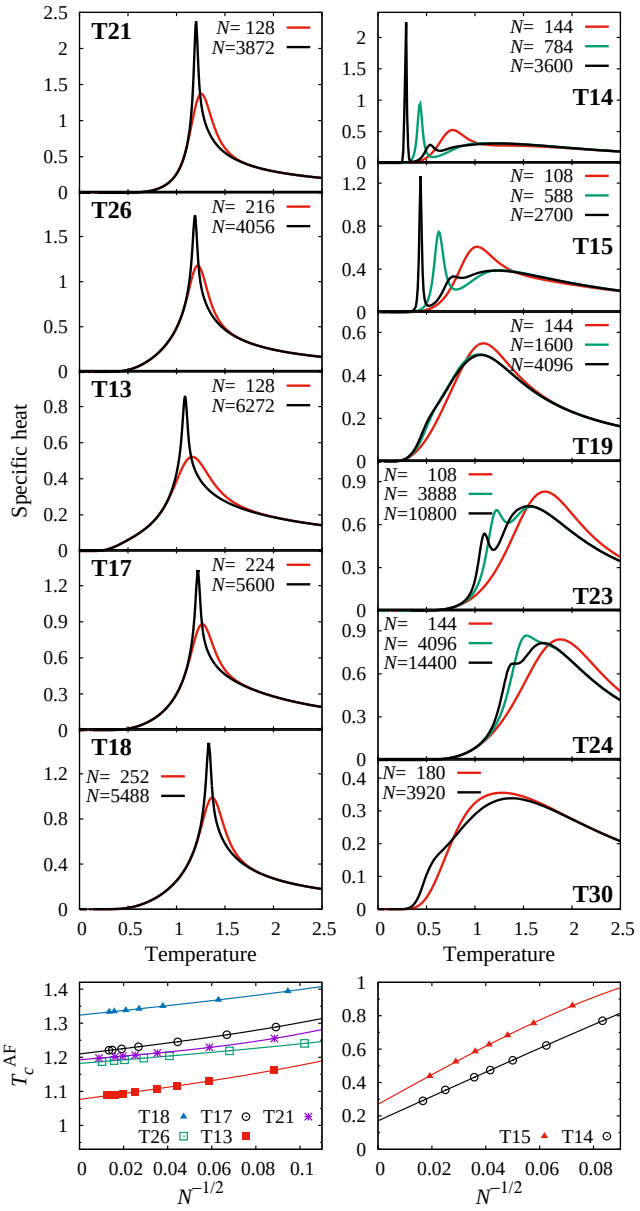

FIG. 2: (Color online) Specific heat as a function of temperature (upper panels) and finite size-scaling to find the critical temperature (lower panels) in the eleven weakly frustrated 2-uniform lattices, which have long-range-ordered ground states. Left and right panels are for lattices with long-range ordering in two and one directions, respectively. Solid lines in the bottom panels are results of fitting for the antiferromagnetic critical temperatures ($T_c^{\rm AF}$) by $T_c^{\rm AF}(N) = T_c^{\rm AF}(\infty) + \lambda N^{-\nu/2}(1 + bN^{-\omega/2})$ with $\nu = 1$ and $\omega = 2$. The temperature is in the unit of $|J|/k_B$.

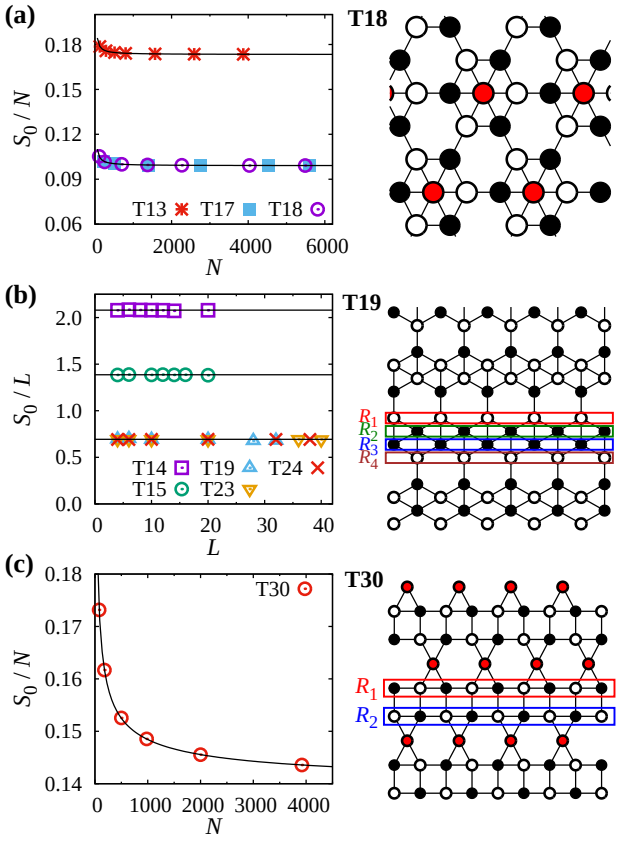

FIG. 3: (Color online) Residual entropy S_0 calculated by the Wang-Landau method for weakly frustrated lattices with long-range-ordered ground state. Lines represent the exact results for each lattice: $S_0 = \log(2)(1 + N/4)$ and $S_0 = \log(2)(1 + N/7)$ in (a), $S_0 = \log(8)L$, $S_0 = \log(4)L$, and $S_0 = \log(2)L$ in (b), and $S_0 = \log(2)(L + N/5)$ in (c). Examples of the ground states for T18, T19, and T30 are shown in the right panels. Black and white circles represent up and down spin sites, respectively. Red circles are for disordered sites with random spin.

a partial order in a few Laves lattices (diced, union jack, and centered diced lattices) [17–19]. As for the Ising model, it was found in the fully-frustrated simple-cubic lattice [20, 21], the stacked triangular lattice [22], the kagome and the bcc lattices with NN and NNN interactions [23, 24], and the anisotropic centered honeycomb lattice [25]. The partial order was also proposed in the quantum Heisenberg model [16, 26] and the periodic Anderson model [27]. Partial order phenomena are also observed experimentally in a few antiferromagnetic materials such as $GdInCu_4$ [28], $Gd_2Ti_2O_7$ [29], and Sr_2YRuO_6 [30].

The five lattices have finite temperature order-disorder transition indicated by diverging specific heat. The temperature of maximum specific heat for various cluster size follows the scaling behavior of the two-dimensional Ising universality class [31]:

$$T_c^{\rm AF}(N) = T_c^{\rm AF}(\infty) + \frac{\lambda}{N^{\nu/2}}\left(1 + \frac{b}{N^{\omega/2}}\right) \qquad (4)$$

with $\nu = 1$ and $\omega = 2$. The two variables λ and b are lattice-dependent fitting parameters. By this method, the critical temperatures were obtained as shown in Fig. 2 and Table I.

The other six lattices (T14, T15, T19, T23, T24, and T30) have the long-range order only in one direction like the Trellis lattice [6]. For example, T19 is made by stripes, each of which is composed of four rows. (See right panel of Fig. 3(b).) In the ground state, all the rows are ordered with the same spin in the horizontal direction. The spins of the first (R_1) and the second (R_2) rows are uniquely determined by the spin of the last row of its adjacent stripe. However, the third (R_3) and the fourth (R_4) rows may choose one between up-down or down-up spins. In other words, when the spin of R_1 is fixed to be up, there are two degenerate spin configurations: up-down-up-down and up-down-down-up for R_1, R_2, R_3, and R_4. Since each stripe has the degeneracy of two, the residual entropy becomes $S_0 = \log\left(2^L\right) = \log(2)L$. By the same reason, the residual entropies of T23 and T24 are also $S_0 = \log(2)L$. T14 and T15 have degeneracy of 2^3 and 2^2 per unit stripe and their residual entropies are $S_0 = \log(8)L$ and $S_0 = \log(4)L$, respectively. As shown in Fig. 3(c), T30 has a partial long-range order in one direction. When R_1 is ordered as $\uparrow\downarrow\uparrow\downarrow\uparrow\downarrow\cdots$, adjacent R_2 should be ordered as $\downarrow\uparrow\downarrow\uparrow\downarrow\uparrow\cdots$. Thus, each stripe composed of R_1 and R_2 has a degeneracy of two. Sites between the two stripes (red circles in Fig. 3(c)) may have any spin and they have degeneracy of two per site. Therefore, the residual entropy of T30 becomes $S_0 = \log(2)(L + N/5)$.

As shown in Fig. 2, specific heat data of T14 and T15 behave similar to the Trellis lattice. They show size-independent broad peak and size-dependent sharp diverging peak at lower temperature, where the one-direction ordering occurs. The temperature of maximum specific heat fits well with Eq. (4) to give the critical temperature of $T_c^{\rm AF} = 0.17(1)$ and $0.27(1)$ for T14 and T15, respectively. Differently from the trellis lattice, the critical exponents ν and ω are the same as the two-dimensional Ising model within statistical error. As for T19, T23, T24, and T30 no finite temperature phase transition was found.

The other nine lattices were found to be disordered even at zero temperature. Their specific heat data as a function of temperature are shown in Fig. 4. They do not have a diverging peak and the size-dependence is very small, which implies absence of long-range correlation. Clearer evidence is the residual entropy, which is proportional to the number of spins within the cluster. They are plotted in Fig. 5 and listed in Table I. Some of them can be calculated analytically. A unit cell of T16 includes seven spins, which makes a hexagon with an extra central spin. (See Fig. 5(b).) Without a central spin (red circle), there is no frustration and the six spins have spin configuration of $(\uparrow\downarrow\uparrow\downarrow\uparrow\downarrow)$ or $(\downarrow\uparrow\downarrow\uparrow\downarrow\uparrow)$. Neighboring hexagons prefer to have different spin configuration with each other, but it is not always possible because they form a triangular lattice. Thus, the residual entropy by hexagons per unit cell is the same as the triangular lattice (T1). Since the central spin may have any direction without changing the energy, it gives extra residual entropy to the lattice. Therefore, the residual entropy is $S_0^{\rm T16}/N = [S_0^{\rm T1}/N + \log(2)]/7$. The residual entropy of the triangular lattice $S_0^{\rm T1}$ is exactly known: $S_0^{\rm T1}/N = (3/\pi)\int_0^{\pi/6}\log(2\cos w)dw \approx 0.32307$ [32]. The residual entropy of T27 and T29 can be understood by the Pauling's method applied to the ice [33]. This method gives approximate but very accurate estimation in corner-sharing frustrated systems [6]. For example, the residual entropy of the kagome lattice (corner-sharing triangles) can be estimated by $S_0^{\rm T8} \approx \log\left[2^N(6/8)^{2N/3}\right] \approx 0.50136N$ [34], where $(6/8)$ means six states out of 2^3 states give minimum energy within a triangle and $2N/3$ means number of triangles in the lattice. This value is smaller than the exact result by 0.1% [35]. In the case of T27, a unit cell, which is star-shaped, is connected with neighboring unit cells with unfrustrated links (thick red lines in Fig. 5(c)). When the two spins connected by unfrustrated links are merged, T27 is transformed into T27*, which has the same residual entropy per unit cell as T27. The residual entropy of T27* is estimated by $S_0^{\rm T27^*} \approx \log\left[2^N(82/2^8)^{N/6}\right] \approx 0.50340N$. $(82/2^8)$ means only 82 states out of 2^8 states satisfy the minimum energy condition in a star-shaped cluster composed of eight spins. Since T27 and T27* have the same residual entropy per unit cell, $S_0^{\rm T27} = (6/8)S_0^{\rm T27^*} \approx 0.37755$. The same method can be applied to T29. By merging four spins connected by square-shaped unfrustrated links, T29

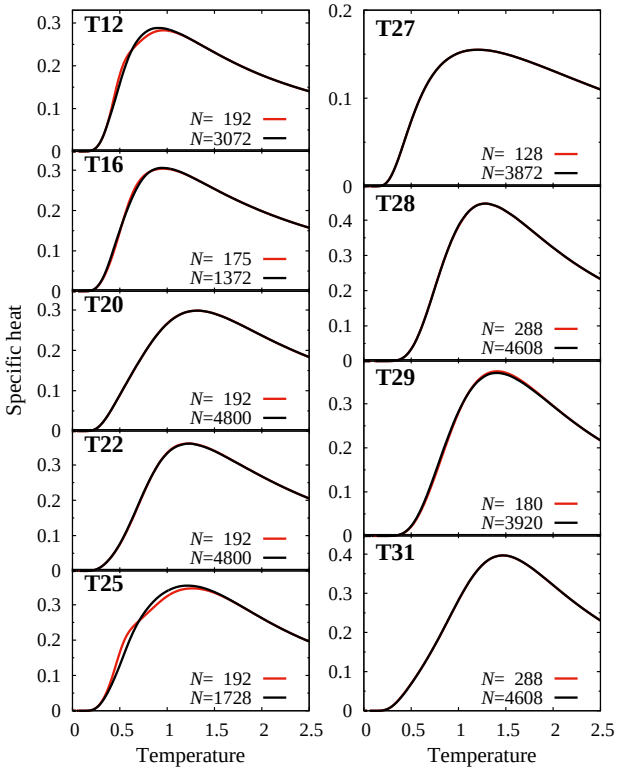

FIG. 4: (Color online) Specific heat as a function of temperature for the nine strongly frustrated 2-uniform lattices.

is transformed into T29*. (See Fig. 5(d).) The residual entropy of T29 is estimated by $S_0^{\mathrm{T29}} = (2/5)S_0^{\mathrm{T29}^*} \approx (2/5)\log\left[2^N(10/2^4)^{N/2}\right] \approx 0.18326$. These estimations are smaller than the numerical results by the Wang-Landau algorithm by 0.005% and 0.3% for T27 and T29, respectively. The other six lattices (T12, T20, T22, T25, T28, and T31) are too complicated to get analytic results or Pauling's estimates. They are in-between 0.08 and 0.18 per spin, which is about half of that of the triangular lattice. This is because there are some unfrustrated links, which reduce the residual entropy of the lattice relative to the triangular lattice. Thick red links in Fig. 5(b)-(d) are examples.

Another important property to study for frustrated systems is the freezing. Spins are frozen in the spin glass phase and the spin ice phase, as well as in the long-range-ordered phase. When spins are not frozen and fluctuate even at zero temperature, it is called the spin liquid. Since DOS does not give information about freezing phenomena, we performed another simulation using the single-site update of the Metropolis algorithm [14]. The degree of freezing can be measured by the Edwards-Anderson order parameter q_{EA} [36], which was proposed to study freezing phenomena in spin glass systems. It can be used generally to study freezing phenomena including the spin ice. We adopted the implementation of Ref. 37:

$$q_{\mathrm{EA},i} = \frac{1}{M}\left|\sum_t^M S_i(t)\right|, \tag{5}$$

$$q_{\mathrm{EA}} = \frac{1}{N}\sum_i^N q_{\mathrm{EA},i}\ . \tag{6}$$

M is the number of Monte-Carlo steps for measurement after equilibration, which is fixed to be $M = 2\times10^6$ in this work. The spin to be tested for flipping is chosen randomly, and each spin is tested once per one Monte-Carlo step on average. At high temperature, spins fluctuate fast and $q_{\mathrm{EA}} \approx 0$. Except the spin liquid, it begins to increase at the transition temperature T_c or freezing temperature T_f as temperature is lowered. For lattices with long-range-ordered ground state (T21, T26, T14, T15, T19, T23, and T24) and spin ice ground state (T20, T22, T25, and T28), all the spins are frozen and q_{EA} approaches 1 at zero temperature. For lattices with partially-long-range-ordered ground state (T13, T17, T18, and T30), spins are frozen except disordered spins and q_{EA} approaches a value in-between zero and one. For example, q_{EA} approaches 6/7 in T18 as temperature goes to zero. No spin liquid ground state was found among the 2-uniform lattices.

Finally we found a new phase, partial spin ice, which appears in T12, T16, T27, T29, and T31, where majority spins are frozen at zero temperature without long-range order, but the other spins are fluctuating. In Fig. 6, $q_{\mathrm{EA},i}$ is shown for T12 and T16. Disordered spins can be connected to make a string like T12 or isolated like T16.

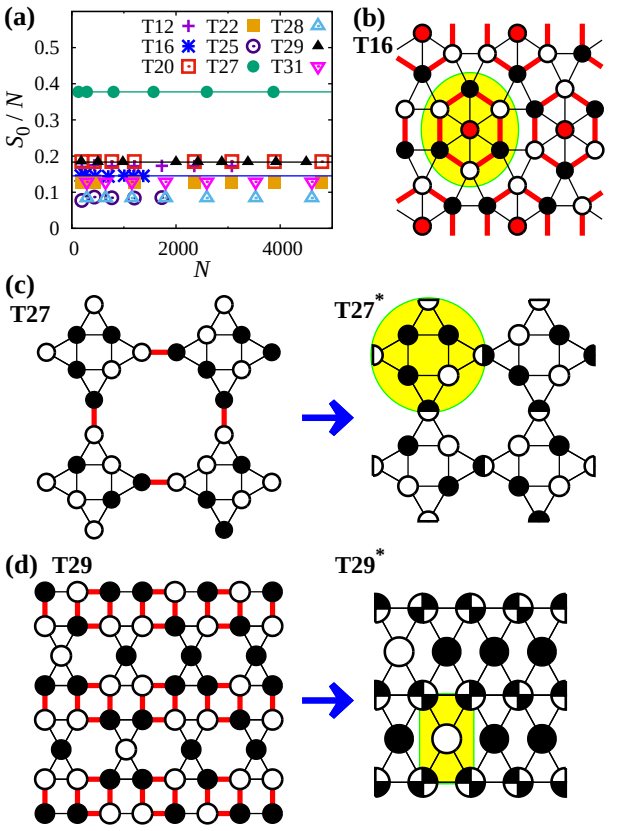

FIG. 5: (Color online) (a) Residual entropy for the 9 strongly frustrated 2-uniform lattices. Horizontal solid lines are $S_0/N = \log(20.5)/8$, $\log(2.5)/5$, and $(0.32306595 + \log(2))/7$ for T27, T29, and T16, respectively. (b) A ground state for T16. Black, white, and red circles represent sites with up-spin, down-spin, and disordered sites. Thick red lines indicate unfrustrated links. (c) and (d) show examples of ground states for T27 and T29. By merging the unfrustrated links (thick red lines), they can be transformed into T27* and T29*, which have the same residual entropy per unit cell as T27 and T29, respectively. Yellow ellipses in (b), (c), and (d) show unit cells.

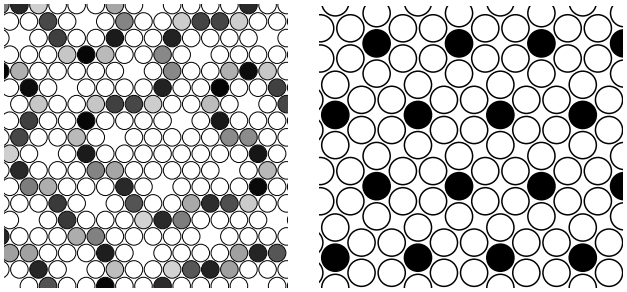

FIG. 6: Freezing order parameter $q_{\mathrm{EA},i}$ at $T = 0.0001$ for T12 (left) and T16 (right) in the partial spin ice phase. White, gray, and black circles represent frozen sites ($q_{\mathrm{EA},i} = 1$), slowly fluctuating sites, and quickly fluctuating sites ($q_{\mathrm{EA},i} = 0$), respectively.

Since frozen region is larger and spans the whole lattice, it would be natural to consider them as a spin ice with exceptional fluctuating parts, and we named them as the partial spin ice.

The ground states of seven frustrated Archimedean lattices and twenty 2-uniform lattices are shown with their ground state energy per bond $E_g^{\rm AF}$ and the coordination number z in Fig. 7. Higher $E_g^{\rm AF}$ and smaller z indicates stronger frustration and tends to induce spin liquid ground state [9, 38, 39]. To the contrary, lattices with lower $E_g^{\rm AF}$ and larger z tend to have a long-range-ordered ground state. In-between, spin ice, partial spin ice, and partial long-range-ordered ground states exist. The general trend is confirmed as shown in Fig. 7, but we found it is not an absolute criterion. T7 (bounce lattice), T26, and T28 have the same coordination number and ground state energy per bond, but T7 and T28 have spin ice ground state while T26 has long-range-ordered ground state.

IV. SUMMARY

We studied systematically the geometric frustration effect of the Ising antiferromagnet on the 2-uniform lattices. From the results of specific heat, residual entropy, and freezing order parameter, we classified ground states of them into long-range order, partial long-range order, spin ice, and partial spin ice. In comparison with the Archimedean lattices [6], partial long-range order and partial spin ice phase were additionally found but spin liquid phase is missing. Table I summarizes the results.

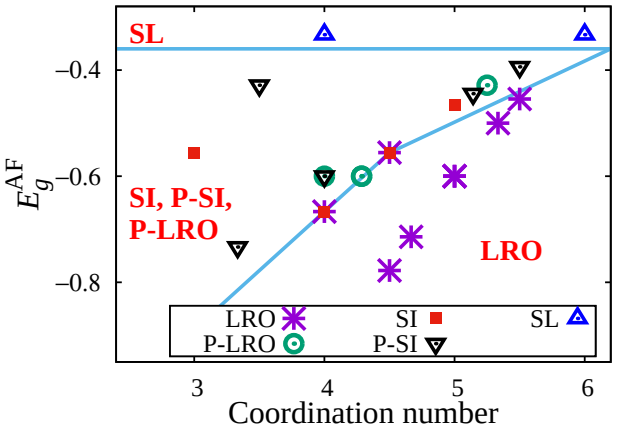

FIG. 7: (Color online) Ground states of the Ising antiferromagnet on twenty seven frustrated Archimedean and 2-uniform lattices represented with their ground state energy per bond $E_g^{\rm AF}$ and the coordination number z. Lower-right corner and upper region indicate weak and strong frustration, respectively. LRO, P-LRO, SI, P-SI, and SL means long-range order, partial long-range order, spin ice, partial spin ice, and spin liquid, respectively.

Acknowledgments

This work was supported by the GIST Research Institute (GRI) in 2016.

[1] L. Balents, Nature **464**, 199 (2010).
[2] H. T. Diep, *Frustrated Spin Systems* (World Scientific, Singapore, 2013), 2nd ed.
[3] C. Lacroix, P. Mendels, and F. Mila, eds., *Introduction to Frustrated Magnetism*, vol. 164 of *Springer Series in Solid-State Sciences* (Springer, New York, 2011).
[4] E. Ising, Z. Phys. **31**, 253 (1925).
[5] R. E. Peierls, Proc. Cambridge Philos. Soc. **32**, 477 (1936).
[6] U. Yu, Phys. Rev. E **91**, 062121 (2015).
[7] A. P. Ramirez, Annu. Rev. Mater. Sci. **24**, 453 (1994).
[8] B. Grünbaum and G. C. Shephard, *Tilings and Patterns* (W. H. Freeman and Company, New York, 1987).
[9] J. Richter, J. Schulenburg, and A. Honecker, in *Quantum Magnetism*, edited by U. Schollwöck, J. Richter, D. J. J. Farnell, and R. F. Bishop (Springer, Berlin, 2004), vol. 645 of *Lecture Notes in Physics*.
[10] D. J. J. Farnell, O. Götze, J. Richter, R. F. Bishop, and P. H. Y. Li, Phys. Rev. B **89**, 184407 (2014).
[11] M. J. Krawczyk, K. Malarz, B. Kawecka-Magiera, A. Z. Maksymowicz, and K. Kułakowski, Phys. Rev. B **72**, 024445 (2005).
[12] Y. Z. Zheng, Z. Zheng, and X. M. Chen, Coord. Chem. Rev. **258-259**, 1 (2014).
[13] F. Wang and D. P. Landau, Phys. Rev. Lett. **86**, 2050 (2001).
[14] N. Metropolis, A. W. Rosenbluth, M. N. Rosenbluth, A. M. Teller, and E. Teller, J. Chem. Phys. **21**, 1087 (1953).
[15] O. Nagai, S. Miyashita, and T. Horiguchi, Phys. Rev. B **47**, 202 (1993).
[16] C. Santamaria and H. T. Diep, J. Appl. Phys. **81**, 5276 (1997).
[17] R. Kotecký, J. Salas, and A. D. Sokal, Phys. Rev. Lett **101**, 030601 (2008).
[18] Q. N. Chen, M. P. Qin, J. Chen, Z. C. Wei, H. H. Zhao, B. Normand, and T. Xiang, Phys. Rev. Lett. **107**, 165701 (2011).
[19] M. P. Qin, Q. N. Chen, Z. Y. Xie, J. Chen, J. F. Yu, H. H. Zhao, B. Normand, and T. Xiang, Phys. Rev. B **90**, 144424 (2014).
[20] D. Blankschtein, M. Ma, and A. N. Berker, Phys. Rev. B **30**, 1362 (1984).
[21] H. T. Diep, P. Lallemand, and O. Nagai, J. Phys. C: Solid State Phys. **18**, 1067 (1985).
[22] D. Blankschtein, M. Ma, A. N. Berker, G. S. Grest, and C. M. Soukoulis, Phys. Rev. B **29**, 5250 (1984).
[23] P. Azaria, H. T. Diep, and H. Giacomini, Phys. Rev. Lett. **59**, 1629 (1987).
[24] P. Azaria, H. T. Diep, and H. Giacomini, Europhys. Lett.

9, 755 (1989).
[25] H. T. Diep, M. Debauche, and H. Giacomini, Phys. Rev. B **43**, 8759 (1991).
[26] R. Quartu and H. T. Diep, Phys. Rev. B **55**, 2975 (1997).
[27] S. Hayami, M. Udagawa, and Y. Motome, J. Phys. Soc. Jpn. **80**, 073704 (2011).
[28] H. Nakamura, N. Kim, M. Shiga, R. Kmiec, K. Tomala, E. Ressouchek, J. P. Sanchezk, and B. Malaman, J. Phys.: Condens. Matter **11**, 1095 (1999).
[29] J. R. Stewart, G. Ehlers, A. S. Wills, S. T. Bramwell, and J. S. Gardner, J. Phys.: Condens. Matter **16**, L321 (2004).
[30] E. Granado, J. W. Lynn, R. F. Jardim, and M. S. Torikachvili, Phys. Rev. Lett. **110**, 017202 (2013).
[31] A. Pelissetto and E. Vicari, Phys. Rep. **368**, 549 (2002).
[32] G. H. Wannier, Phys. Rev. **79**, 357 (1950).
[33] L. Pauling, J. Am. Chem. Soc. **57**, 2680 (1935).
[34] R. Liebmann, *Statistical Mechanics of Periodic Frustrated Ising Systems*, vol. 251 of *Lecture Notes in Physics* (Springer-Verlag, Berin, 1986).
[35] K. Kanô and S. Naya, Prog. Theo. Phys. **10**, 158 (1953).
[36] S. F. Edwards and P. W. Anderson, J. Phys. F: Metal Phys. **5**, 965 (1975).
[37] V. T. Ngo, D. T. Hoang, H. T. Diep, and I. A. Campbell, Mod. Phys. Lett. B **28**, 1450067 (2014).
[38] S. Kobe and K. Handrich, Phys. Stat. Sol. B **73**, K65 (1976).
[39] S. Kobe and T. Koltz, Phys. Rev. E **52**, 5660 (1995).